J. Biochem. **139**, 881–885 (2006)
doi:10.1093/jb/mvj101

Mutations of Ferritin H Chain C-Terminus Produced by Nucleotide Insertions Have Altered Stability and Functional Properties

Rosaria Ingrassia, Gianmario Gerardi, Giorgio Biasiotto and Paolo Arosio*
Dipartimento Materno Infantile e Tecnologie Biomediche, Università di Brescia, A.O. Spedali Civili, Viale Europa 11, 25123 Brescia, Italy

Received December 21, 2005; accepted March 18, 2006

Ferritin is an iron storage protein made of 24 subunits. Previous mutational analyses showed that ferritin C-terminal region has a major role in protein stability and assembly but is only marginally involved in the mechanism of iron incorporation. However, it has recently been shown that patients who carry alterations of ferritin C-terminal sequence caused by nucleotide insertions show neurological disorders possibly related to altered protein functionality and cellular iron deregulation. To re-evaluate the role of this region, five mutants of mouse H-ferritin were produced by 2-nucleotide insertions that modified the last 6–29 residues and extended the sequence of 14 amino acids. The mutants were expressed in *Escherichia coli* and analysed for solubility, stability and capacity to incorporate iron. The alteration of the last 6-residue non-helical extension had no evident effect on the properties of ferritin, while solubility and capacity to assemble in ferritin shells decreased progressively with the extension of the modified region. The results also showed that the modification of even a part of the terminal E-helix abolished the capacity of ferritin to incorporate iron during expression in the cells, probably caused by conformational modification of the hydrophobic channels. The data support the hypothesis that the pathogenic mutations alter cellular iron homeostasis.

Key words: ferritin, hereditary ferritinopathies, iron metabolism, iron uptake, protein folding.

Ferritin, a ubiquitous iron storage molecule, is mostly cytosolic in vertebrates and composed of H and L chains (*1*, *2*). The two subunits co-assemble in variable proportions to form 24-mer ferritin shells. The H chain has a ferroxidase activity that facilitates iron incorporation and is essential for cellular iron regulation and detoxification (*3*, *4*). The L chain has no enzymatic activity on its own, but contributes to ferritin functionality by presenting sites that facilitate iron nucleation and mineralization and improves the activity of ferroxidase centres (*5*). Ferritin has a highly conserved structure from bacteria to human, and each subunit folds in a 4-helical bundle (helices A–D), with a long loop connecting helices B and C, plus a fifth short E helix at the C-terminus. The mechanism of iron incorporation involves ferroxidase centres localized inside the bundle, hydrophilic pores on the three-fold symmetry axis, and residues exposed on the cavity for iron nucleation/mineralization (*1*). The functional role of these sites has been verified by a large number of site-specific mutations, mainly on recombinant ferritin H-types (*5–10*). Various mutants have also been produced to modify the C-terminal region, including the last segment of the D-helix, the DE turn, the short E-helix and the non-helical terminal extension (*6*, *7*, *11–13*). They were found to be less soluble and to show folding/assembly problems, because of the alteration of residues involved in the contacts along the 4-fold symmetry axes, where four subunits come together. Of these mutants, those that formed ferritin shells showed ferroxidase and iron incorporation capacity only slightly lower than wild-type ferritin (*6*, *7*), indicating that this region is not directly involved in ferritin iron incorporation. The exceptions were the mutants deleted of the E-helix or with the C-terminus fused to large peptides, which were unable to incorporate detectable iron in the cavity (*6*, *7*). Recently it was shown that heterozygous nucleotide insertions in exon 4 of L-ferritin are associated with neurodegeneration in the basal ganglia of the brain, with the formation of large cytosolic and intranuclear protein bodies positive for ferritin, iron and ubiquitin (*14–16*). The observed cellular iron accumulation found in these hereditary ferritinopathies may not be caused only by abnormal ferritin folding and aggregation, but also by alteration of ferritin functionality, resulting in cellular iron deregulation (*17–19*). The one or two-nucleotide insertions modify the last 28, 22 and 9 residues of L-ferritin, which are substituted by new, unrelated sequences that extend the peptides of 4 and 13 residues. Particularly intriguing is the 498InsTC of the L-ferritin, which modifies only 9 C-terminal residues (5 of the E-helix and 4 non-helical) with the extension of 14 new amino acids, which may be predicted to be buried inside ferritin cavity (*15*). Previous mutational data give little insight into the structural and functional effects of these modifications, since they were mostly based on the analysis of point substitutions or of truncations. Therefore, we produced similar mutations in the ferritin H-chain, which has the advantage over the L-ferritin of having ferroxidase

*To whom correspondence should be addressed. Tel: +39-030 394 386, Fax: +39-030-307 521, E-mail: arosio@med.unibs.it

activity and therefore being more easily amenable to functional studies. The results indicate that the longer the mutated sequences the higher is the effect on protein solubility and assembly. They also show that the modification of even a portion of the E-helix inhibits the capacity of ferritin to incorporate iron in vivo. This supports the hypothesis that the pathogenic mutations of L-ferritin found in hereditary ferritinopathies may affect ferritin functionality.

MATERIALS AND METHODS

Ferritin Mutation, Expression—Before performing the mutageneses, we cloned into the pET vector the full-length MoFTH cDNA including 40 bp of the 3′UTR up to 90 bp upstream of the polyadenylation site. The 589 bp fragment was obtained by RT-PCR from mouse liver total RNA, in a 1-h reaction at 42°C with 200 units of Superscript RNAseH (Invitrogen) using the reverse primer 5′AGATTATCggatccTCAGTGACCAGTAAAGTCACGTG3′, which carries a *Bam*HI site (lower case). The fragment was then PCR amplified using the forward primer 5′AGATTATCcatatgACCACCGCGTCTCCCTCG3′ with *Nde*I site (lower case) and the same reverse primer to obtain the 616 bp amplicon. The fragment was purified and inserted into the *Nde*I–*Bam*HI sites of pET12a vector (Novagen). The construct, named pET-MoHF-3′UTR, was verified by DNA sequencing; it encodes the full-ferritin cDNA and the 3′UTR up to 589 bp.

The mutageneses were performed using Quick Change site-directed mutagenesis method (Stratagene) according to the manufacturer's instructions. The following mutated oligonucleotides were used for each mutant (the inserted nucleotides are underlined): *529insTC-FOR*: 5′TTTGACAAGCACACCCTGTCGGACACGGTGATGAGAGCTA3′, and *529insTC*-REV, for –6 mutant; *509insTC-FOR*: 5′CTGGCATGGCAGAATATCTCTCTTTGACAAGCACACCCTG3′ and *509insTC-REV*, for –12 mutant; *497insTC-FOR*: 5′GCCCCTGAAGCTGGCATCTGGCAGAATATCTCTT3′, and *497insTC-REV*, for –17 mutant; *475insTC-FOR*: 5′CGTGACCAACTTACGCAAGTCATGGGTGCCCCTGAAGCTG3′, and *475insTC-REV*, for mutant –24; *460insAC-FOR*: 5′AGAACTGGGTGACCACGTGACACCAACTTACGCAAGATGGGT3′, and the anti-sense *460insAC-REV*, for mutant –29; *P161stop-FOR*: 5′ACTTACGCAAGATGGGTGCCTAAGAAGCTGGCATGGCAGAATA3′, and *P161stop-REV*, with codon substitution for deletion mutant 161X (–21X). Mutations were verified by DNA sequencing. The plasmids were used to transform *E. coli* strain BL21(DE3) (Novagen). The cells were grown at 37°C until an optical density of 0.7 at 600 nm, then expression was induced by addition of 0.4 mM IPTG (Isopropyl-β-D-thiogalactopyranoside) (Sigma-Aldrich) and the cells grown for another 3 h. The cells were harvested and disrupted by sonication, and the homogenates were separated into soluble and insoluble fractions by centrifugation at 14,000 × *g* for 20 min. The precipitates were resuspended in buffer to a volume equal to that of the soluble fraction. Protein content was evaluated by BCA protein assay (Pierce).

Analytical Methods—Electrophoreses were carried in 7.5% non-denaturing PAGE, and 12% SDS-PAGE. Gels were stained with Coomassie Blue. Western Blotting was performed with a rabbit anti-mouse ferritin heavy chain (anti-MoHF) (*19*) at 1:1,000 dilution, followed by HRP-labelled anti rabbit IgG antibody, and the bound activity revealed by ECL (EuroClone). In some experiments the samples were concentrated on Amicon Ultra-4 Centrifugal Filter devices, 10.000 MWCO (Millipore).

Thermodynamic stability of the mutants was evaluated by pulse proteolysis with various concentrations of urea, according to the method described in Ref. *20*, using thermolysin (typeX, from *Bacillus thermoproteolyticus rokko*, SIGMA-ALDRICH). Briefly, the soluble extracts (about 0.15 mg/ml of specific protein) were equilibrated overnight at room temperature in various concentrations of Urea in 0.1 M sodium acetate pH 5.5, 10 mM $CaCl_2$. Thermolysin (0.3 mg/ml, final concentration) was then added at the sample for 1 min at 37°C and the reaction stopped by additions of 2.5 μl 0.1 M EDTA (pH 8.0). The samples were then analysed on 12% SDS PAGE.

Iron Incorporation—Ferritin iron was stained with Prussian blue reaction using 2% potassium ferrocyanide in 10% HCl (*21*). In the experiments to monitor iron incorporation capacity, the proteins were separated on non-denaturing PAGE, blotted on nitrocellulose filter (Hybond P, Amersham), the filters were equilibrated in 0.1 M Hepes pH 6.5, and then incubated for 2 h with 200 μM ferrous ammonium sulphate (FAS) in 0.1 M Hepes, pH 6.5. After washing, the iron incorporated into ferritin was revealed by Prussian Blue reaction.

RESULTS

A two-nucleotide insertion in mouse H-ferritin (MoFTH) cDNA alters the downstream sequence and introduces an extension of 14 residues, a length very similar to that of the pathogenic 498InsTC mutation of human L-ferritin (13 residues). Human H-ferritin was not chosen because the same insertions produce a shorter extension (11 residues) that has no higher homology to that of the pathogenic mutant. Thus, we generated six MoFTH mutants by inserting TC, in position 529–530, 509–510, 497–498, 475–476 and AC in position 460–461, which altered the sequence from codons –6, –12, –17, –24 and –29, respectively, numbering from the C-terminus (Fig. 1). The insertions modified the last 6 non-helical residues, the terminal half or the whole E-helix, the DE turn and the last part of the D-helix, respectively. The new sequences that result from the frameshift mutations have no homology with that of the native protein and eliminate most of the acidic groups, with a large increase in the hydrophobicity of the region, introducing up to three tryptophans. Secondary structure predictions using NPS@GOR4 (http://npsa-pbil.ibcp.fr/cgi-bin/npsa_automat.pl?page=npsa_gor4.html) program indicated that the new sequences lost the propensity to form helical structures but gained that to form strand structures. Finally, we analysed a mutant truncated at proline 161 (–21X), which lacks the DE turn and E-helix.

Protein Expression—The six mutants were expressed with similar efficiency in *E. coli*. The homogenates were fractionated into soluble and insoluble fractions, and SDS-PAGE showed that the proportion of soluble ferritins decreased progressively on moving the insertion upstream (Fig. 2A, lanes S), while that of the insoluble

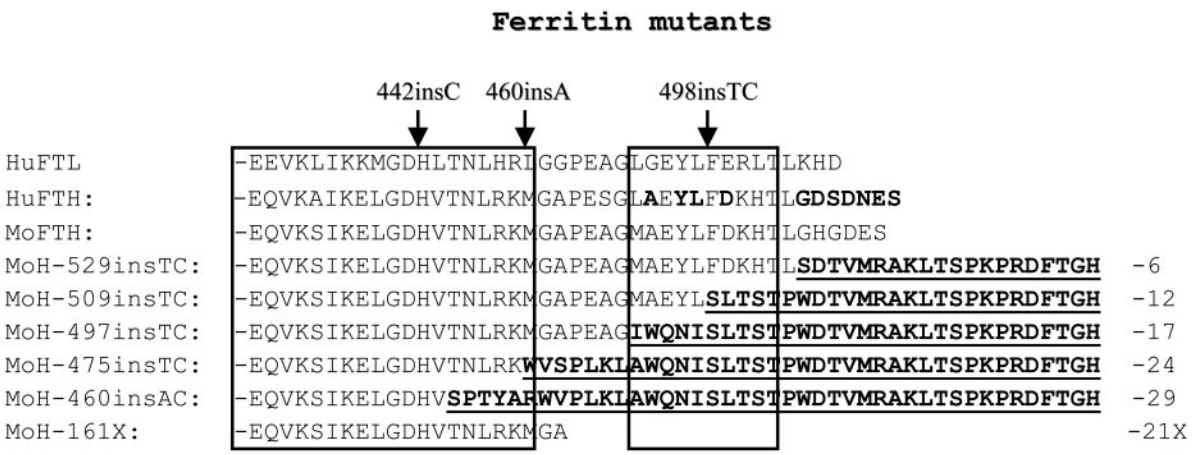

Fig. 1. **Sequence alignment of human L-ferritin, human and mouse H-ferritin and mutants.** The C-terminal sequence of human FTL (HuFTL) and human FTH (HuFTH) is aligned with that of mouse FTH (MoFTH) and its mutants. The nucleotide insertions in the mRNAs are indicated on the left, and the short codes used in the work are indicated on the right of the sequences. The substitutions are underlined. The HuFTH residues modified in previous works (*6*, *7*) are in bold, and the D-helix and E-helix are boxed. The localization of the frame shift mutations of human L-ferritin found in hereditary ferritinopathies is indicated with vertical arrows.

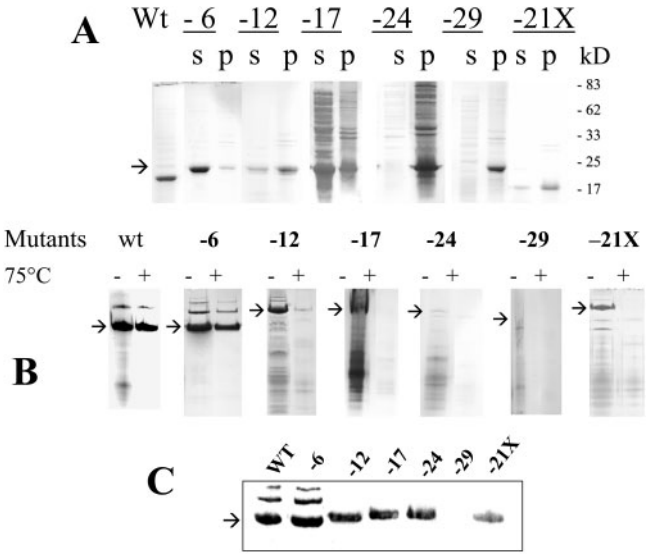

Fig. 2. **Electrophoretic analysis of the mutants.** Panel A: The soluble (S) and insoluble fractions (P) of the mutants indicated were brought to the same volumes, and 7 μl of each was analysed on SDS-PAGE in comparison with MoFTH-wt (WT). Coomassie Blue stain. Panel B: The soluble extracts of the indicated mutants before (–) and after a treatment at 75°C for 20 min (+) analysed on non-denaturing PAGE, stained with Coomassie Blue. The arrows point to the bands of the assembled ferritin shells. Panel C: Western blotting with anti-MoFTH antibody. About 4 μg of the soluble fractions of the indicated mutants was resolved on non-denaturing PAGE, blotted with antibody diluted 1:1,000, and visualized with ECL.

protein increased (Fig. 2A, lanes P). In particular, mutant –6 was mostly soluble, like MoFTH, while mutants –24 and –29 were found only in the insoluble fraction (Fig. 2A). The trend was confirmed by non-denaturing PAGE, which showed that assembled ferritin shells were present in the soluble extracts of mutants –6, –12, –17, and –21X, but not in those of mutants –24 and –29 (Fig. 2B). More sensitive immunoblotting detected a minor proportion of assembled –24 only after concentration of the soluble fractions, but not of mutant –29 (Fig. 2C). This also showed that mutants –12, –17 and –24 had slightly slower mobility than MoFTH, while mutant –6 had the same pattern as MoFTH, including the typical bands of dimers and oligomers. Since the insolubility of the mutants may be caused by aggregation of ferritin shells or of unfolded peptides, we analysed the insoluble fraction of the homogenates. Assembled ferritins were found to account for a high proportion of the precipitates of mutants –12, –17 and –21X, evident after resolubilization in buffer and in 4 M urea (Fig. 3A). At the highest possible urea concentration (9 M), the ferritin band decreased, probably because of partial denaturation. Assembled ferritins were not detectable in the insoluble fractions of mutants –24 and –29 (not shown), indicating that they do not fold and assemble efficiently during expression in *E. coli*. Since the recovery of these two mutants was very low, they were not characterized any further.

Mutant Stability and Resistance to Proteolysis—The resistance to 75°C heating, which is a typical ferritin property, was conserved only in mutant –6, and not in mutants –12, –17 and –21X (Fig. 2B: lanes +). In an other approach, the soluble fractions of MoFTH and mutants –6, –12, –17 and –21X were equilibrated for 18 h with various concentrations of urea, and then subjected to a 1-min pulse with excess thermolysin, which digests only the unfolded domains of the protein (*20*). Mutant –6 was unaffected by the treatment, while the mutants –12, –17 and –21X were partially digested in the intermediate (3–6 M) and the highest possible urea concentration (8 M, Fig. 3B).

Iron Incorporation—The major function of ferritin is to incorporate iron both *in vivo* and *in vitro*. To evaluate if the mutants retained these functions, the concentrated soluble fractions of the homogenates were separated on

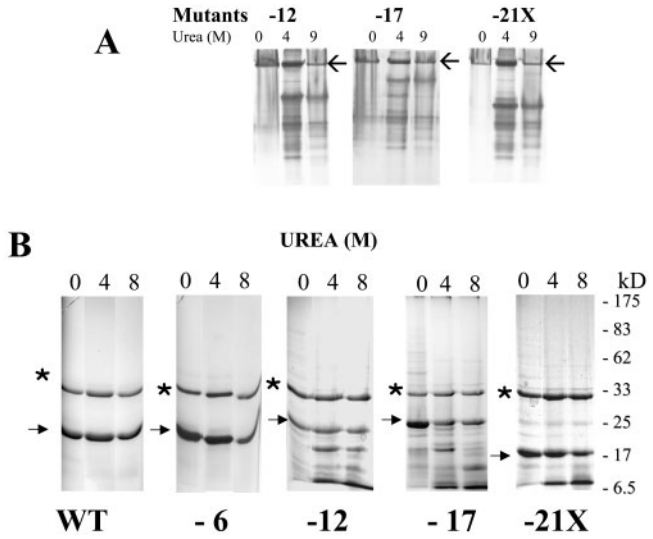

Fig. 3. **Solubility and resistance to proteolysis.** Panel A: Equal amounts of the insoluble fractions of indicated mutants were resuspended in Tris-HCl buffer (pH 7.5) containing 0 M, 4 M or 9 M Urea and then analysed on non-denaturing PAGE, followed by Coomassie Blue staining. The arrows indicate the assembled ferritin shells. Panel B: about 5 μg of the indicated ferritin mutants was equilibrated for 18 h at room temperature with various concentrations of urea (0, 4, 8 M), incubated for 1 min at 37°C with thermolysin (0.3 mg/ml final concentration), and then separated on SDS-PAGE. The asterisks show thermolysin bands, and the arrows indicate the bands of ferritin subunits. Coomassie Blue stain.

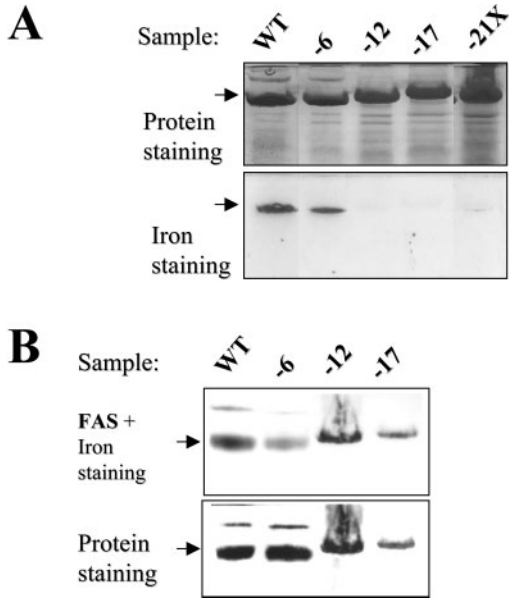

Fig. 4. **Iron Incorporation.** Panel A: About 25 μg of the soluble fractions of the indicated proteins was separated on non-denaturing PAGE and stained with Prussian Blue (iron stain), followed by Coomassie Blue staining (protein stain). The arrows indicate the assembled ferritin shells. Panel B: About 2 μg of the soluble mutant proteins was separated on non-denaturing PAGE, transferred onto a nitrocellulose filter, incubated for 2 h with 200 μM ferrous ammonium sulphate (FAS) in 0.1 M Hepes pH 6.5, and the iron incorporated into ferritin stained with Prussian Blue (iron stain). The proteins on the filter were stained with Ponceau Red (Protein stain). The arrows indicate the ferritin shells.

non-denaturing PAGE and stained with Prussian Blue. As expected, MoFTH developed a positive staining, as did mutant –6. In contrast, mutants –12, –17 and –21X did not, indicating that they are unable to incorporate iron during the expression in *E. coli* (Fig. 4A). However, under the more favourable *in vitro* conditions, when the ferritins were incubated aerobically with Fe(II) salts at pH 6.5, all mutants, including –12 and –17, incorporated iron and could be stained with Prussian Blue (Fig. 4B).

DISCUSSION

The present data show that mutant –6 had very similar properties to the MoFTH, implying that neither the non-helical C-terminal extension nor the 14 residue extension affected ferritin assembly or iron incorporation capacity. Similar findings were previously observed with a mutant deleted of the same non-helical sequence (*6*), or with the C-terminus fused to a short 26 amino acid sequence (*22*). Thus, the non-helical sequence is not involved in important stability interactions, and 14–26 residue extensions can be buried inside the cavity. In contrast mutant –12 was less soluble than MoFTH, and the ferritin shells showed lower heat stability and proteolysis resistance. This may suggest that the last two turns of the E-helix (residues –6 to –12) carry interactions that stabilise the protein and facilitate its assembly. However, the only described human H-ferritin (HuFTH) mutant affecting this sequence D171→Y (which correspond to –11D→Y in MoFTH) behaved like normal ferritin (*6*, *7*) as did mutants HuFTH-Y168D and A166D (which correspond to –14Y→D and –16A→D in MoFTH) (*6*, *7*). A significant effect on ferritin solubility and stability was observed in mutant HuFTH-L169R (–13L→R in MoFTH), which introduces a bulky and charged residue that is expected to disrupt the hydrophobic interactions stabilizing the 4-fold channels (*6–8*). This mutant was reported to have normal functionality in iron incorporation, while the present mutant-12 does not, since it is unable to incorporate iron during expression in *E. coli*. Interestingly, the lack of this property was observed in the mutant truncated of the whole E-helix (–21X) and in those with the C-terminus fused to a large peptide that inhibited the burying of the E-helix in the cavity (*6*, *7*). This observation suggests that the modification of residues –6 to –12 perturbs the folding of the whole E-helix, inducing important conformational modifications of the channel that affect ferritin functionality. This hypothesis is supported by the finding that the mutant is accessible to proteolysis producing peptides with size compatible with the cleavage of E-helix. In mutant –17, the E-helix is fully modified, and thus the structural modifications that affect the channel and functionality are even more important, and in fact it also did incorporate iron *in vivo*. More dramatic results are produced by a further extension of the frameshift to –24 and –29 residues, which abolish the complete E-helix, the DE turn and some of the distal D-helix, and strongly reduced ferritin assembly and functionality. It should be noted that the mutants lost the capacity to incorporate iron during expression in *E. coli*, *i.e.*, in an environment

that is close to the physiological one of the mammalian cellular cytosol. Ferritins must be fully functional to incorporate detectable iron under these conditions, where iron availability is low and tightly controlled by cellular systems that include the endogenous ferritins. In contrast, a minor residual activity is sufficient to incorporate iron in the *in vitro* conditions we used, where iron is much more abundant and available. The finding that the mutants incorporate iron *in vitro* indicates that they retained a shell-like structure with some functionality.

In conclusion, the present data indicate that the relevant modifications in the frameshift mutants of ferritin C-terminus are those affecting the helical structure of the molecule, they reduce not only protein folding/assembly, but also the major function of the molecule, which is to sequester cellular iron. In contrast, the 14 nucleotide extension does not appear have a major effect on folding or functionality. We believe that these data have some implication for the interpretation of the pathogenic mutations of human L-ferritin, which interest the same region we have analysed . The new sequences introduced by the frameshifts in MoFTH, human L-ferritin, and by 1 or 2-nucletide insertions, have no homology, but they share the effect of disrupting the native helical structure. Therefore, we propose that the three pathogenic mutations, even the L-ferritin 498InsTC, modify not only ferritin folding, but also its functionality to incorporate iron *in vivo*, and support the hypothesis that hereditary ferritinopathies are associated with cellular iron mishandling (*23*).

The financial support of Telethon Italy (grant GGP05141) is gratefully acknowledged. The work was partially supported by MIUR-Firb and Cofin-04 grants to PA. We are grateful to Dr S. Levi and Dr. P. Cavadini for helpful comments.

REFERENCES

1. Harrison, P.M. and Arosio, P. (1996) The ferritins: molecular properties, iron storage function and cellular regulation. *Biochim. Biophys. Acta* **1275**, 161–203
2. Arosio, P. and Levi, S. (2002) Ferritin, iron homeostasis, and oxidative damage(1,2). *Free Radic Biol Med.* **33**, 457–463
3. Ferreira, C., Bucchini, D., Martin, M.E., Levi, S., Arosio, P., Grandchamp, C., and Beaumont, C. (2000) Early embryonic lethality of H-ferritin gene deletion in mice. *J. Biol. Chem.* **275**, 3021–3024
4. Cozzi, A., Corsi, B., Levi, S., Santambrogio, P., Albertini, A., and Arosio, P. (2000) Overexpression of wild type and mutated human ferritin H-chain in HeLa cells: in vivo role of ferritin ferroxidase activity. *J. Biol. Chem.* **275**, 25122–25129
5. Levi, S., Yewdall, S.J., Harrison, P.M., Santambrogio, P., Cozzi, A., Rovida, E., Albertini, A., and Arosio, P. (1992) Evidence that H and L-ferritins have co-operative roles in the iron uptake mechanism of human ferritin. *Biochem. J.* **288**, 591–596
6. Levi, S., Luzzago, A., Franceschinelli, F., Santambrogio, Cesarei, G., and Arosio, P. (1989) Mutational analysis of the channel and loop sequences of human ferritin H-chain. *Biochem. J.* **264**, 381–388
7. Levi, S., Luzzago, A., Cesareni, G., Cozzi, A., Franceschinelli, F., Albertini, A., and Arosio, P. (1988) Mechanism of ferritin iron uptake: activity of the H-chain and deletion mapping of the ferro-oxidase site. A study of iron uptake and ferro-oxidase activity of human liver, recombinant H-chain ferritins, and of two H-chain deletion mutants. *J. Biol. Chem.* **263**, 18086–18092
8. Levi, S., Santambrogio, P., Albertini, A., and Arosio, P. (1993) Human ferritin H-chains can be obtained in non-assembled stable forms which have ferroxidase activity. *FEBS Lett.* **336**, 309–312
9. Liu, X. and Theil, E.C. (2004) Ferritin reactions: direct identification of the site for the diferric peroxide reaction intermediate. *Proc. Natl. Acad. Sci. USA* **101**, 8557–8562
10. Liu, X., Jin, W., and Theil, E.C. (2003) Opening protein pores with chaotropes enhances Fe reduction and chelation of Fe from the ferritin biomineral. *Proc. Natl. Acad. Sci. USA* **100**, 3653–3658
11. Luzzago, A. and Cesareni, G. (1989) Isolation of point mutations that affect the folding of the chain of human ferritin in *E. coli*. *EMBO J.* **8**, 569–576
12. Jappelli, R., Luzzago, A., Tasateo, P., Pernice, I., and Cesareni, G. (1992) Loop mutations can cause a substantial conformational change in the carboxy terminus of the ferritin protein. *J. Mol. Biol.* **227**, 532–543
13. Jappelli, R. and Cesareni, G. (1996) Loop mutations affect ferritin solubilità causing non-native aggregation of subunits or precipitation of fully assembled polymers. *FEBS Lett.* **394**, 311–315
14. Curtis, A.R.J., Fey, C., Morris, C.M., Bindoff, L.A., Ince, P.G., Chinnery, P.F., Coulthard, A., Jackson, M.J., Jackson, A.P., McHale, D.P., Hay, D., Barker, W.A., Markham, A.F., Bates, D., Curtis, A., and Burn, J. (2001) Mutation in the gene encoding ferritin light polypeptide causes dominant adult-onset basal ganglia disease. *Nature Genet.* **28**, 350–354
15. Vidal, R., Ghetti, B., Takao, M., Brefel-Courbon, C., Uro-Coste, E., Glazier, B.S., Siani, V., Benson, M.D., Calvas, P., Miravalle, L., Rascol, O., and Delisle, M.B. (2004) Intracellular ferritin accumulation in neural and extraneural tissue characterizes a neurodegenerative disease associated with a mutation in the ferritin light polypeptide gene. *J. Neuropathol. Exp. Neurol.* **63**, 363–380
16. Mancuso, M., Davidzon, G., Kurlan, R.M., Tawil, R., Bonilla, E., Di Mauro, S., and Powers, J.M. (2005) Hereditary ferritinopathy: a novel mutation, its cellular pathology, and pathogenetic insights. *J. Neuropathol. Exp. Neurol.* **64**, 280–294
17. Crompton, D.E., Chinnery, P.F., Fey, C. *et al*. (2002) Neuroferritinopathy: a window on the role of iron in neurodegeneration. *Blood Cells Mol. Dis.* **29**, 522–531
18. Vidal, R., Delisle, M.B., and Ghetti, B. (2004) Neurodegeneration caused by proteins with an aberrant carboxyl-terminus. *J. Neuropathol. Exp. Neurol.* **63**, 787–800
19. Levi, S., Cozzi, A., and Arosio, P. (2005) Neuroferritinopathy: a neurodegenerative disorder associated with L-ferritin mutation. *Best Pract. Res. Clin. Haematol.* **18**, 265–276
20. Park, C. and Marqusee, S. (2005) Pulse proteolysis: a simple method for quantitative determination of protein stability and ligand binding. *Nat. Methods* **2**, 207–212
21. Santambrogio, P., Cozzi, A., Levi, S., Rovida, E., Magni, F., Albertini, A., and Arosio, P. (2000) Functional and immunological analysis of recombinant mouse H- and L-ferritins from *Escherichia coli*. *Protein Expr. Purif.* **19**, 212–218
22. Gerardi, G., Biasiotto, G., Santambrogio, P., Zanella, I., Ingrassia, R., Corrado, M., Cavadini, P., Derosas, M., Levi, S., and Arosio, P. (2005). Recombinant human hepcidin expressed in *Escherichia coli* isolates as an iron containing protein. *Blood Cells Mol. Dis.* **35**, 177–181
23. Cozzi, A., Santambrogio, P., Corsi, B., Campanella, A., Arosio, P., and Levi, S. (2006) Characterization of the L-ferritin variant 460InsA responsible of a neuroferritinopathy disorder. submitted